Available online at www.sciencedirect.com

SCIENCE DIRECT

Biochimica et Biophysica Acta 1711 (2005) 12–19

BIOCHIMICA ET BIOPHYSICA ACTA BBA

http://www.elsevier.com/locate/bba

Molecular associations and surface-active properties of short- and long-*N*-acyl chain ceramides

Jesús Sot, Félix M. Goñi, Alicia Alonso*

Unidad de Biofísica (Centro Mixto CSIC-UPV/EHU), and Departamento de Bioquímica, Universidad del País Vasco, Aptdo. 644, 48080 Bilbao, Spain

Received 13 September 2004; received in revised form 21 February 2005; accepted 22 February 2005
Available online 16 March 2005

Abstract

The behaviour of *N*-hexadecanoylsphingosine (Cer16), *N*-hexanoylsphingosine (Cer6) and *N*-acetylsphingosine (Cer2) in aqueous media and in lipid–water systems, monolayers and bilayers has been comparatively examined using Langmuir balance and fluorescence techniques. Cer16 behaves as an insoluble non-swelling amphiphile, not partitioning into the air–water interface, thus not modifying the surface pressure of the aqueous solutions into which it is included. By contrast both Cer6 and Cer2 behave as soluble amphiphiles, up to approx. 100 μM. At low concentrations, they become oriented at the air–water interface, increasing surface pressure in a dose-dependent way up to ca. 5 μM bulk concentration. At higher concentrations, the excess ceramide forms micelles, critical micellar concentrations of both Cer6 and Cer2 being in the 5–6 μM range. When the air–water interface is occupied by a phospholipid, Cer2 and Cer6 become inserted in the phospholipid monolayer, causing a further increase in surface pressure. This increase is dose dependent, and reaches a plateau at ca. 2 μM ceramide bulk concentration. Both Cer2 and Cer6 become inserted in phospholipid monolayers with initial surface pressures of up to 43 and 46 mN m^{-1}, respectively, which ensures their capacity to become inserted into cell membranes whose monolayers are estimated to support a surface pressure of about 30 mN m^{-1}. Both Cer2 and Cer6, but not Cer16, had detergent-like properties, such as giving rise to phospholipid–ceramide mixed micelles, when added to phospholipid monolayers or bilayers. The short-chain ceramides form large aggregates and precipitate at concentrations above approx. 100 μM. These results are relevant in cell physiology studies in which short- and long-chain ceramides are sometimes used as equivalent molecules, in spite of their different biophysical behaviour.

Keywords: Ceramide; Short-chain ceramide; Amphiphile; Surfactant; Detergent; Lipid monolayer; Surface pressure; Bilayer solubilization; Micelle

1. Introduction

The discovery of the sphingolipid signalling pathway of cell metabolism [1,2] has increased the interest of biophysicists in the properties of ceramides, or *N*-acyl sphingosines, in membranes (for reviews, [3–5]). Ceramides have been found in nature with *N*-fatty acyl chains containing from 2 to 28 carbon atoms. Those with C16 to C24 fatty acids are most common, although ceramides containing C2 to C6 fatty acids are frequently used in experimentation. Extensive biophysical work has been performed with the long-*N*-acyl chain ceramides, while the properties of the "short-chain ceramides" (i.e. short-*N*-acyl chain ceramides) have been comparatively less studied [6,7].

Long-*N*-acyl chain ceramides are highly hydrophobic and essentially insoluble and non-dispersible in water. In phospholipid bilayers, one outstanding property of long-chain ceramides is their strong tendency to separate laterally in the plane of the membrane giving rise to distinct ceramide-rich and phospholipid-rich domains [8–14]. The property of lateral phase separation appears to be at the origin of the conversion of the sphingolipid, cholesterol-rich

Abbreviations: ANS, 1-anilinonaphthalene-8-sulfonic acid; Cer2, *N*-acetylsphingosine; Cer6, *N*-hexanoylsphingosine; Cer16, *N*-hexadecanoylsphingosine; cmc, critical micellar concentration; DEPE, dielaidoylphosphatidylethanolamine; DMSO, dimethylsulfoxide; MLV, multilamellar vesicles; NBD-SM, 6-((*N*-(7-nitrobenz-2-oxa-1, 3-diazol-4-yl)amino)hexanoyl)sphingosylphosphocholine; PC, phosphatidylcholine; Rh-PE, *N*-(lissamine rhodamine B sulfonyl) phosphatidylethanolamine

* Corresponding author. Tel.: +34 94 601 26 25; fax: +34 94 601 33 60.
E-mail address: gbpaliza@lg.ehu.es (A. Alonso).

0005-2736/$ - see front matter © 2005 Elsevier B.V. All rights reserved.
doi:10.1016/j.bbamem.2005.02.014

transient microdomains known as "rafts" into large-scale, long-lived platforms involved in signal transduction, by effect of sphingomyelinase activity (for reviews, [4,15]). The same property of long-chain ceramides may be at the origin of the recently described displacement of cholesterol from ordered lipid domains by ceramide [16]. Short-*N*-acyl chain ceramides in turn can be easily dispersed in water, and they do not give rise to in-plane phase separation [7]. Simon and Gear [6] demonstrated that *N*-acetylsphingosine (Cer2) caused platelet fenestration and ultimately platelet lysis, in a detergent-like manner.

In view of the above data, we have undertaken a study of the surface-active and self-association properties of ceramides in aqueous media, with the aim of providing a molecular understanding of the current observations. Both long-chain (*N*-palmitoylsphingosine, Cer16) and short-chain (*N*-acetylsphingosine, Cer2; *N*-hexanoylsphingosine, Cer6) ceramides have been used. The surface-active properties of ceramides have also been explored. Self-association in aqueous environments has been tested through the ceramide ability to form micelles. Our studies show that long-chain ceramides belong in the category of "insoluble non-swelling amphiphiles" in the classification of Small [17], implying that they cannot give rise to micelles or other hydrated aggregates in water suspension, while short-chain ceramides, at least at concentrations below 100 μM, behave as "soluble amphiphiles" in the same classification, i.e. "detergents" as defined by Helenius and Simons [18], giving rise to micelles in water and solubilizing phospholipid monolayers and bilayers.

2. Materials and methods

Egg PC, DEPE, Cer16, Cer6 and Cer2 were supplied by Avanti Polar Lipids (Alabaster, AL). ANS, NBD-SM, and Rh-PE were from Molecular Probes (Alabaster, AL). All lipids were >98% pure as supplied and were used without further purification. All other reagents were of analytical grade.

The study of the surface properties of monomolecular lipid layers at the air–water interface was carried out using a μTrough-S equipment (Kibron, Helsinki, Finland) at 25 °C under constant stirring and constant monolayer area of 3.14 cm^2. The aqueous subphase consisted of 1 ml 20 mM PIPES, 150 mM NaCl, 1 mM EDTA, pH 7.4. Phospholipids dissolved in chloroform:methanol (2:1,v/v) were gently spread over the surface until the desired initial surface pressure was attained. The ceramides (in less than 50 μl DMSO) were either deposited on top of the aqueous phase or injected into the subphase with a Hamilton microsyringe through a hole connected to the subphase. The solubilization of Rh-PE monolayers by ceramides was assayed by measuring rhodamine fluorescence emission (excitation at 530 nm, emission at 590 nm) of the subphase in a SLM-Aminco 8100 spectrofluorimeter.

The critical micellar concentrations (cmc) of the ceramides were measured [19] as an increase in 5 μM ANS fluorescence emission (excitation at 390 nm and emission at 550 nm) in 20 mM PIPES, 150 mM NaCl, 1 mM EDTA, pH 7.4, at room temperature (21 ± 1 °C). Fluorescence measurements were carried out in a SLM-AMINCO 8100 spectrofluorometer.

For liposome preparation, lipids were dissolved in cloroform:methanol (2:1,v/v), and the solvent evaporated exhaustively. Multilamellar vesicles (MLV) were prepared by hydrating the dry lipids in buffer, with vortex shaking. Lipids were hydrated in 20 mM PIPES, 150 mM NaCl, 1 mM EDTA, pH7.4. Final concentration was measured as lipid phosphorus. Liposome suspensions were mixed with the appropriate ceramide suspensions in DMSO. The final liposome concentration was 100 μM in phospholipid. The mixtures were left to equilibrate for 24 h at room temperature. The suspension light scattering was measured in a SLM-AMINCO 8100 spectrofluorometer at room temperature, with excitation and emission wavelengths set at 520 nm. The solubilization of DEPE or egg PC liposomes by ceramides was measured as follows: 1 ml MLV (100 μM) were treated with 5 μl of the appropriate ceramide in DMSO, with stirring. The suspensions were left to equilibrate for 24 h, after which the mixtures were centrifuged in an Eppendorf centrifuge at 14,500 rpm, 4 °C, 20 min. The clear supernatant was considered to contain the solubilized fraction, that was quantified by determining lipid phosphorous.

When required, the experimental data were fitted to either hyperbolic or sigmoidal curves using the Sigmaplot software.

3. Results

3.1. Ceramide–water systems

The surface-active properties of the ceramides were first tested in a Langmuir balance. Ceramides (in DMSO solution) were either deposited on top of the interface or injected into the subphase, and the change in surface pressure (π) was recorded. DMSO alone did not cause any significant change in π. The representative curves of ceramide effects are shown in Fig. 1. For Cer16 (Fig. 1A), the addition on top of the buffer surface causes an immediate increase in π, that remains afterwards constant. This constant value is operationally defined as an equilibrium value in this context. The injection of Cer16 into the subphase does not cause any change in π. A different situation is found for Cer2 (Fig. 1B). Whatever the mode of dispensation, this ceramide partitions between the subphase and the interface, and the same operational equilibrium value of π (ca. 6 mN m^{-1} for a 1 μM bulk concentration of Cer2) is measured. When different concentrations of Cer2 or Cer6 are injected into the

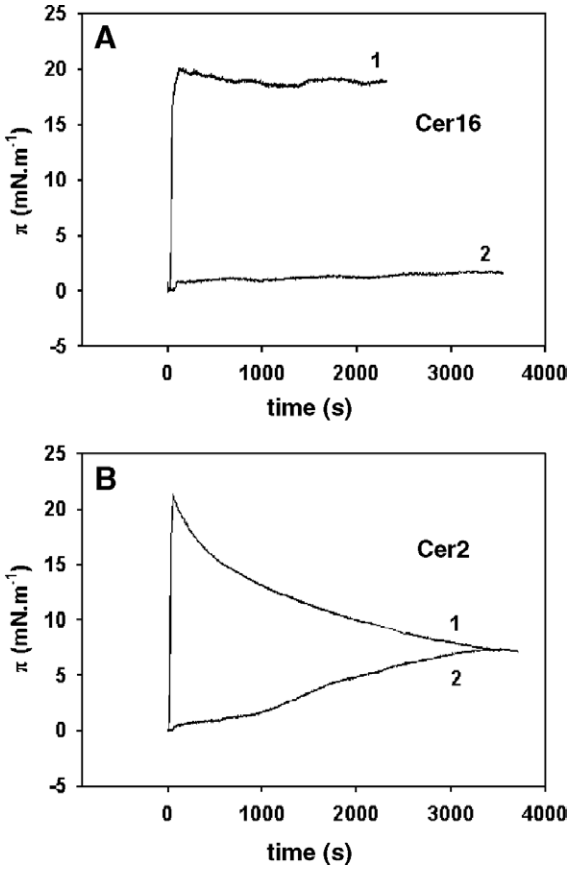

Fig. 1. Time course of ceramide-induced changes in surface pressure at an air–water interface. Subphase composition was 20 mM PIPES, 150 mM NaCl, 1mM EDTA, pH 7.4. Ceramides in DMSO solution were either deposited onto the water surface (curves 1) or injected into the subphase (curves 2). (A) Cer16. (B) Cer2. The amounts of added ceramide correspond to bulk concentrations of 2 μM (Cer16, curve 1), 10 μM (Cer16, curve 2), and 1 μM (Cer2, both curves).

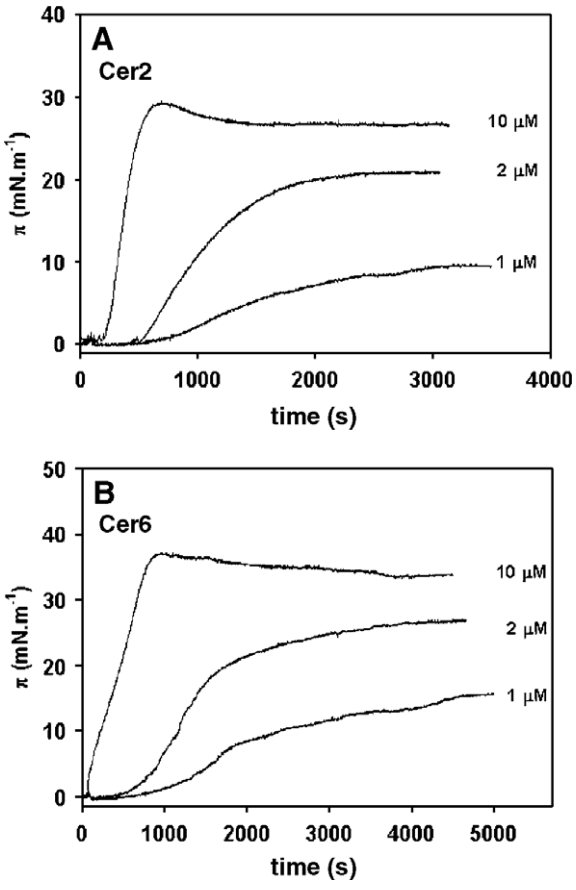

Fig. 2. Time course of short-chain ceramide-induced changes in surface pressure at an air–water interface. Subphase composition was 20 mM PIPES, 150 mM NaCl, 1 mM EDTA, pH 7.4. Ceramides were injected into the subphase in the DMSO solution. Time courses are shown for the surface pressure changes induced by various concentrations of ceramide. (A) Cer2. (B) Cer6.

subphase, a dose-dependent increase in π is observed (Fig. 2). Equilibrium is reached only after 1–2 h, with Cer6 taking longer than Cer2. At ceramide concentrations above 5 μM, a maximum surface pressure is achieved shortly after injection, then π values decrease slowly to their equilibrium values. This represents probably a fast ceramide partitioning to the interface, followed by a slow dispersion in the bulk water (see below). Thus, it appears as if Cer16 is not present at the surface compared to Cer2 and Cer6 which induce a much larger change of surface pressure at lower bulk concentrations. However, this may not be quantitatively exact considering that Cer16 forms a very condensed film [13] while films of Cer2 and Cer6 should be liquid expanded and have a much larger cross-sectional mean molecular area than Cer16 does. This means that, compared to Cer16, a smaller number of molecules of Cer2 and Cer6 should lead to a larger change of surface pressure by adsorption onto a same surface area.

The dose-dependent character of the surface pressure increase due to short-chain ceramide partitioning into the air–water interface is seen in more detail in Fig. 3. This

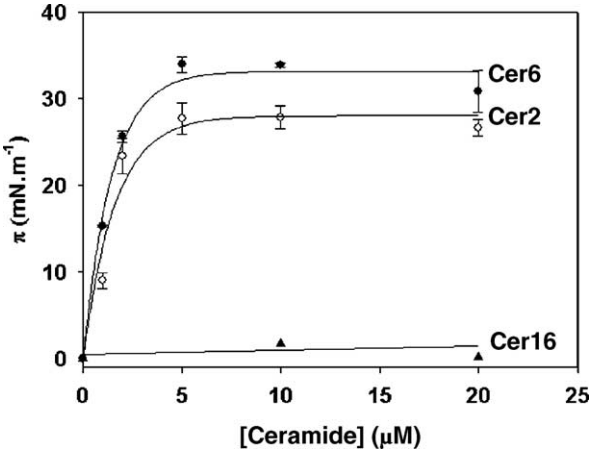

Fig. 3. Equilibrium values of ceramide-induced changes in surface pressure at an air–water interface. Data are obtained from experiments as those shown in Fig. 2. Average values ± S.E. ($n=3$). The curves are hyperbolas; the limit values of π for infinite ceramide concentration are respectively 28 mN m^{-1} (Cer2) and 33 mN m^{-1} (Cer6).

figure shows also that the interface becomes saturated at ca. 5 μM ceramide, and this explains the biphasic curves shown in Fig. 2 for 10 μM Cer2 and Cer6. Once the interface becomes saturated, ceramide molecules start dispersing in the bulk of the solvent, as will be shown below. Cer6 reaches a plateau at a surface pressure ca. 5 mN m^{-1} higher than Cer2. Cer16 does not cause any change in surface pressure when injected into the subphase in the range of concentrations under study. Ceramide-induced increases in surface pressure indicate that the surface becomes stabilized by the spontaneous adsorption of these molecules. However, the observed differences in $\Delta\pi$ caused by the various ceramides do not necessarily refer to the actual number of molecules present at the interface since other factors, e.g. surface electrostatics, may contribute to the observed effects.

The dispersion of short-chain ceramides in aqueous media was studied by examining micelle formation. For soluble amphiphiles, micelles form above a certain concentration (or rather a concentration range), commonly called the "critical micellar concentration" (cmc). A convenient method to observe micellization relies on the fluorescence emission properties of ANS. This molecule has a low fluorescence emission in aqueous environments, but its fluorescence increases markedly, and is shifted to lower wavelengths, when transferred to a less polar environment, such as the micelle core. Thus, by measuring ANS fluorescence emission at increasing ceramide concentrations, the formation of ceramide micelles is observed as an abrupt increase in fluorescence, at the cmc. This is shown in Fig. 4. Panel A depicts the cmc measurements for Cer2 and Cer6. In both cases, the increase in fluorescence shows a discontinuity at 5–6 μM, signalling a cmc in agreement with the surface pressure data in Figs. 2 and 3. Fig. 4B, whose ordinate scale is one order of magnitude larger than that of Fig. 4A, shows for both ceramides a second departure from linearity at ca. 100 μM. The validity of our analysis describing two discontinuities in the "fluorescence vs. log [Cer]" plots was checked by computing the r^2 correlation coefficients of the four regression lines shown in Fig. 4A and the four regression lines shown in Fig. 4B. In all eight cases, $r^2 \geq 0.94$. However, when the data in Fig. 4A were fitted to a single straight lines, i.e. assuming no discontinuities, $r^2 \leq 0.83$. The data in Fig. 4B, when fitted to single straight lines, gave $r^2 \leq 0.57$. We concluded that the experimental data were best interpreted in terms of three straight lines, with discontinuities at ca. 5–6 μM and 100 μM, as indicated by the arrows. Above 100 μM, ceramide aggregation proceeds steadily, as seen from the increase in light scattering by the ceramide dispersions (Fig. 4C). In the 100–1000 μM region of Cer2 and Cer6 concentrations large aggregates are formed that give rise to visible precipitates in the test tube: Above ≈ 100 μM the ceramides start coming out of solution. In summary, (i) at concentrations up to 5–6 μM, Cer2 and Cer6 exist in the form of monomers, (ii) above

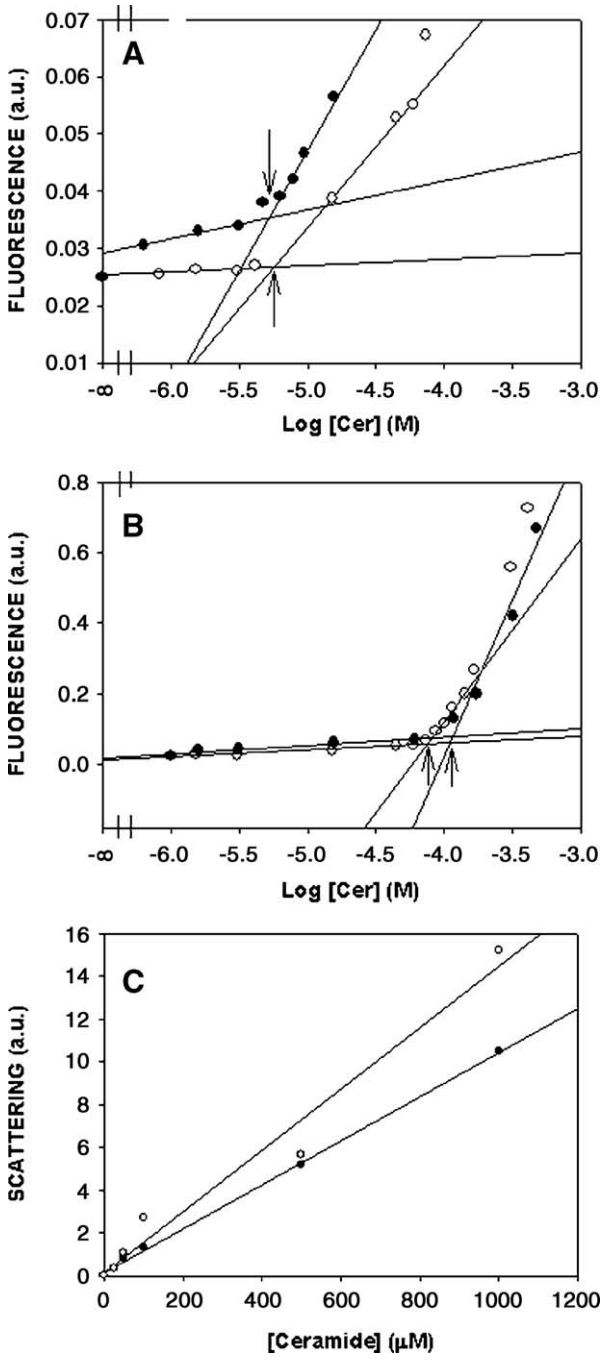

Fig. 4. Critical micellar concentrations (cmc) of short-chain ceramides. The cmc, indicated by the arrows, were estimated from the discontinuities in ANS fluorescence emission as ceramide concentration was increased. (○) Cer2. (●) Cer6. (A) Aggregation (micellization) near the 5 μM concentration region (B) Aggregation near the 50 μM region. Note the different scales in the *Y* axis of Panels A and B. (C) Ceramide aggregation observed as an increase in light scattering of Cer2 and Cer6 dispersions. Average values of two closely similar experiments.

≈ 5 μM, monomer concentration stays constant, with micelle concentration increasing up to ≈ 100 μM, and (iii) above ≈ 100 μM, monomer and micelle concentrations remain constant, the excess ceramide precipitating out of the solution.

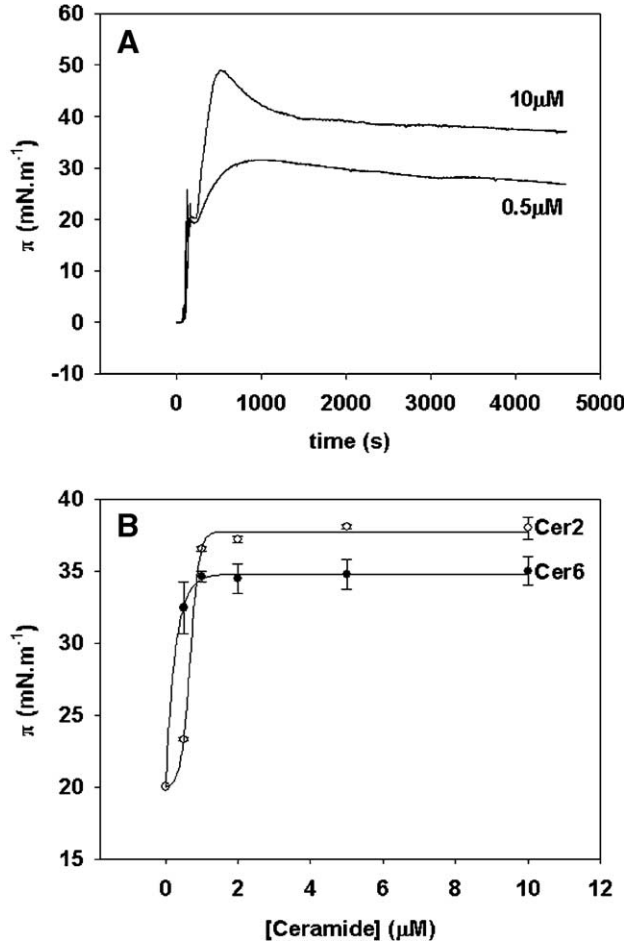

Fig. 5. Insertion of short-chain ceramides into DEPE monolayers oriented at the air–water interface. (A) Two representative time courses of the changes in surface pressure upon the injection of 0.5 μM or 10 μM Cer2 into the subphase and subsequent insertion into the monolayer. (B) Equilibrium values of ceramide-induced surface pressure changes. Subphase composition as in Fig. 1. Average values ± S.E. ($n=3$). Cer6 values were fitted to a hyperbola; the limit π value for infinite ceramide concentration is 34.8 mN m^{-1}. Cer2 values were fitted to a sigmoid curve, of equation $y=y_o+a/1+\exp[-(x-x_o)/b]$, the limit π value for infinite ceramide concentration is 37.7 mN m^{-1}.

3.2. Ceramide–phospholipid–water systems

Soluble amphiphiles such as Cer2 and Cer6 should be considered as "detergents", according to Helenius and Simons [18]. Detergents are able to insert into, and interact with, phospholipid monolayers/bilayers giving rise to detergent–phospholipid mixed micelles. The insertion of the "soluble" Cer2 and Cer6 into phospholipid monolayers was tested using the Langmuir balance, with preformed DEPE monolayers at the air–water interface, and ceramides injected into the water phase. DEPE was chosen as a phospholipid in order to compare our present results with previous [12] and ongoing studies on DEPE-Cer16 mixtures using differential scanning calorimetry. DEPE in excess water exists in the lamellar phase within a wide range of pH and temperatures [20,21], thus it can be considered as representative of most biomembrane phospholipids. Ceramide insertion into a DEPE monolayer at 20 mN m^{-1} increases lateral pressure in a dose-dependent form, as indicated in Fig. 5. The π vs. ceramide concentration curves reach a plateau at ca. 2 μM ceramide. At variance with the ceramide–water system, Cer2 increases π to a larger extent (by ca. 3 mN m^{-1}) than Cer6 does. An additional, perhaps related, difference is that the π vs. Cer2 experimental data fit a sigmoidal curve better than the π vs. Cer6 data does. The insertion of Cer2 into egg PC monolayers caused very similar changes in π (data not shown).

Ceramide insertion-dependent increases in lateral pressure depend strongly on the initial π value. The maximum (plateau) values of surface pressure increase ($\Delta\pi$) after Cer2 and Cer6 insertion are plotted as a function of initial π in Fig. 6. The data can be fitted to straight lines, whose extrapolation to $\Delta\pi=0$ gives an idea of the maximum monolayer surface pressure that allows ceramide insertion into monolayers. Both Cer2 and Cer6 may become inserted into monolayers at initial π above 40 mN m^{-1}. Considering that cell membranes are believed to support a lateral pressure $\pi \approx 30$ mN m^{-1} [22], the data in Fig. 6 would suggest that both Cer2 and Cer6 can insert easily into cell membranes, in agreement with their widespread use in cell biology research. Note in addition that, due to the available thermal energy and depending on the in-plane elasticity of the interface, fluctuations of 10 mN m^{-1} can occur about the average value, and this can probably make easier for many molecules to become inserted in membranes.

The fact that $\Delta\pi$ subsequent to ceramide insertion soon reaches a plateau (Fig. 5), together with the well-known properties of other soluble amphiphiles [18], suggests that short-chain ceramides, above a given concentration, start solubilizing the DEPE monolayers, giving rise to DEPE:-ceramide mixed micelles. This hypothesis was tested using a fluorescent derivative of phosphatidylethanolamine, namely Rh-PE. Preliminary experiments showed that Rh-PE mono-

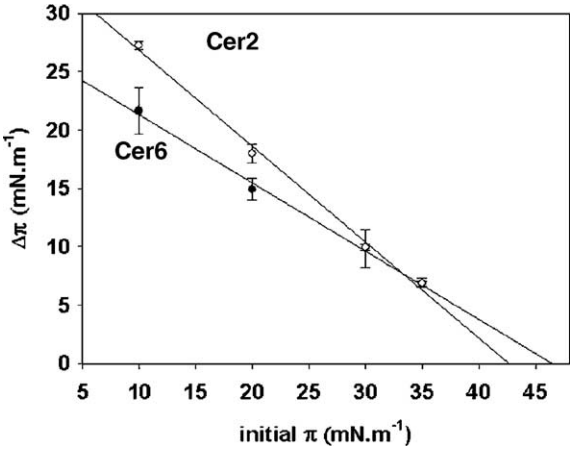

Fig. 6. Changes in surface pressure of DEPE monolayers as a result of ceramide insertion, at varying initial pressures. Average values ± S.E. ($n=3$).

layers behaved just as DEPE monolayers with respect to the π increase in the presence of ceramides (data not shown). Rh-PE monolayers were formed at an initial $\pi = 20$ mN m^{-1} and ceramides were injected into the subphase at 10 μM and 50 μM bulk concentrations. After allowing for equilibration, aliquots of the subphase were withdrawn and rhodamine fluorescence assayed. As shown in Fig. 7, short-chain ceramides, Cer2 in particular, brought about the solubilization of Rh-PE, while Cer16 was inactive in this respect. The presence of Rh-PE fluorescence in the aqueous phase was accompanied by a decrease in surface pressure. Essentially, similar results were obtained when NBD-SM, a fluorescent sphingomyelin derivative that contains the fluorophore in the acyl chain, was used instead of Rh-PE, that is labelled in the headgroup (data not shown), indicating that the fluorescent moiety was not causing substantial changes in the phospholipid surface behaviour.

The ability of Cer2 and Cer6 to solubilize phospholipid bilayers was tested next. For this purpose, MLV composed of DEPE were prepared and mixed with increasing concentrations of ceramide. Final phospholipid concentration was 100 μM, ceramide concentration ranged from 0 to 500 μM. After 24 h incubation at room temperature, the suspensions were centrifuged (see Materials and methods) and lipid phosphorous assayed in the supernatants. The proportion of solubilized P had a maximum at 12% for Cer2, and was even lower for Cer6 (data not shown). The low solubilization was attributed to the fact that, at room temperature, both DEPE and the ceramides are in the gel state. Thus, the solubilization assays were repeated with MLV composed of egg PC. This phospholipid is totally fluid at room temperature, and may be more appropriate to represent the physical state of cell membranes when they are treated with ceramides. The results of the solubilization assays with egg PC are shown in Fig. 8. Dose-dependent solubilization is observed, and again Cer2 data appear to fit more appropriately a sigmoid curve (see Fig. 5). However, complete solubilization of egg PC MLV is not observed even with a 5-fold excess ceramide (data not shown), suggesting a limited tendency of Cer2 and Cer6 to form mixed micelles with the phospholipid.

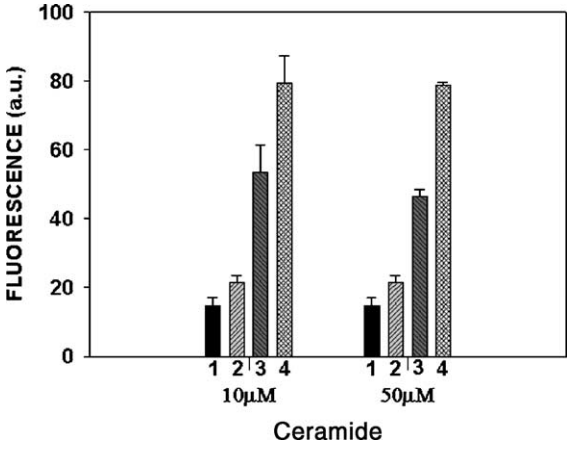

Fig. 7. Solubilization of Rh-PE monolayers by ceramide. Ceramide in the DMSO solution was injected into the subphase of monolayers of fluorescent Rh-PE at an initial $\pi = 20$mN m^{-1}. After equilibration, aliquots of the subphase were removed and rhodamine fluorescence assayed. Final ceramide concentration was 10 μM or 50 μM, as indicated. Column 1: pure DMSO. Column 2: Cer16. Column 3: Cer6. Column 4: Cer2. Average values ± S.E. ($n = 3$).

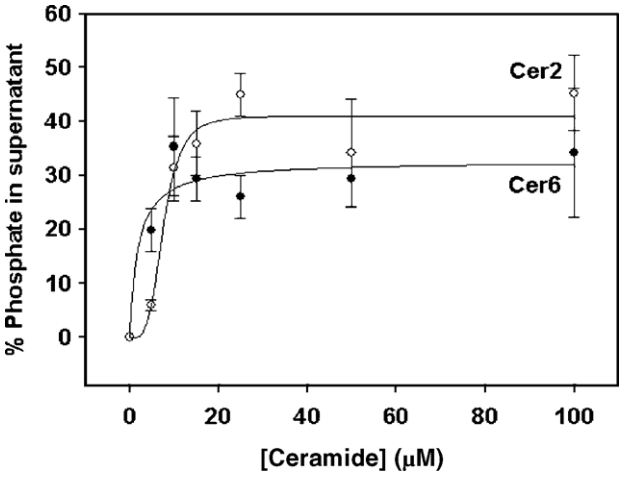

Fig. 8. Ceramide-induced solubilization of egg PC vesicles. Egg PC MLV vesicles (final concentration 100 μM) were incubated with varying concentrations of Cer2 or Cer6. After 24 h equilibration at room temperature, the suspensions were centrifuged and phospholipid assayed in the supernatants. Average values ± S.E. ($n = 3$). Cer6 values were fitted to a hyperbola; the limit π value for infinite ceramide concentration is 32.6 mN m^{-1}. Cer2 values were fitted to a sigmoid curve, of equation $y = y_o + a/1 + \exp[-(x - x_o)/b]$; the limit π value for infinite ceramide concentration is 40.4 mN m^{-1}.

4. Discussion

4.1. Ceramides as amphiphiles

Ceramides should be considered as amphiphiles, because their molecule contains both lipophilic and hydrophilic moieties. Of the former, fatty acyl chain length may vary considerably, acyl chains with 2 to 28 carbon atoms having been found in nature [3,23,24]. In his useful classification of amphiphiles, Small [17] distinguished between non-swelling, swelling and soluble amphiphiles. According to the results in this paper (Figs. 1, 3, and 7), ceramides containing an *N*-fatty acyl residue of at least C16 ("long-chain ceramides") should be classified as insoluble non-swelling amphiphiles. This group of substances, of which diglycerides and triglycerides are common examples, can orient themselves at the air–water interface, but hardly partition into it, i.e. water surface tension is virtually unchanged when they are introduced in the bulk of the solvent [25,26]. This explains, e.g. that C16 ceramide is virtually unable to exchange between membranes, at least without the aid of an exchange protein [27]. In contrast, our results with two "short-chain ceramides", Cer2 and Cer6, in agreement with

some previous observations, reveal a very different behaviour, because they can be easily dispersed in water, up to ≈100 μM, giving rise to optically clear or slightly opalescent dispersions. Thus short-chain ceramides could be classified as "soluble amphiphiles", together with biomolecules such as lysophospholipids or fatty acylcarnitines, and with the commonly called detergents. The property of easy water dispersion has earned the short-chain ceramides a role in cell physiology experimentation, as putative analogues of their more common long-chain counterparts [3,28,29].

4.2. The interpretation of monolayer studies

A number of precautions should be taken when interpreting the results involving surface tension measurements. In particular, the change in surface tension as a result of ceramide addition cannot be considered a direct measurement of the number of ceramide molecules in the interface. This is because of the complex thermodynamics involved in the surface equilibrium regarding interfacial adsorption from bulk solution. According to the Gibbs adsorption equation isotherm, a given decrease or increase in surface tension can be accounted for by changes of the surface concentration of molecules, by changes of the surface chemical potential (which includes interactions and surface electrostatics) and/or by both [22,30,31].

4.3. Short-chain ceramides as detergents

Previous studies by Simon and Gear [6] and by Di Paola et al. [32] described the properties of short-chain ceramides that were not shared by long-chain ceramides, in particular the ability of the former to perturb cell membranes. The results in this paper (Figs. 2, 3, and 4) show that both Cer2 and Cer6 behave as typical soluble amphiphiles, with cmc in the 5 μM range. In comparison, the micellization of lysophosphatidylcholine occurs in the 40–50 μM range, and the corresponding cmc values for palmitoylcarnitine and for Triton X-100 are respectively of ca. 10 μM and 370 μM, these values being rather sensitive to temperature, ionic strength, etc. [33].

Short-chain ceramides are also able to solubilize phospholipids both in the form of monolayers (Figs. 5 and 7) and of bilayers (Fig. 8). Bringing the monolayer lateral tension beyond a certain point is probably a pre-requisite for micelle formation to occur [18,34]. The concentration range of the phenomena described in Figs. 5 and 8 is very different, as befits two different stages in membrane solubilization: Stage I [18], or insertion of detergent monomers, is shown in Fig. 5, while stage II, micelle formation and onset of solubilization, is shown in Fig. 8. At variance with most of the detergents used in biomembrane studies, short-chain ceramides do not achieve complete bilayer solubilization (Fig. 8), even at ceramide:phospholipid mole ratios of 5:1 (data not shown). For egg phosphatidylcholine bilayers, the detergent:phospholipid mole ratio producing full solubilization is of ≈2–3:1 for most, if not all, the biochemically used surfactants [35]. However, under our conditions, lipid concentration was 100 μM (about the lowest that allows reliable solubilization assays using the lipid phosphorous method) and, as mentioned above, 100 μM is also the concentration above which Cer2 and Cer6 start precipitating. Thus, in this system, the available ceramide never exceeds 100 μM, and ceramide:phospholipid ratio is at most 1:1, a ratio that allows only partial solubilization (Fig. 8). This low solubility of Cer2 and Cer6 may also explain that the proportion of solubilized Rh-PE monolayers by 10 and 50 μM ceramide is the same (Fig. 7). Note that the centrifugation data in Fig. 8, by themselves, could also be compatible with a ceramide-induced formation of small unilamellar vesicles containing phospholipid and ceramide, that would not sediment under our centrifugation conditions, even in the absence of true MLV solubilization. However the results in Fig. 7 would not support this interpretation.

4.4. Concluding remarks

Short- and long-chain ceramides represent an interesting family of molecules, with the same chemical groupings, but widely different physical properties derived from the different *N*-acyl lengths. The different lengths lead, in turn, to a different hydrophile–lipophile balance, and probably to a different molecular shape, thus to a different behaviour both in aqueous media and in phospholipid environments, as described in this paper. These observations bear physiological relevance, firstly because both short- and long-chain ceramides appear to exist in cells, although the significance of this remains hitherto unexplored, and also because in experimental cell physiology, short-chain ("soluble") ceramides are used for convenience when the physiological effects of the more abundant long-chain ceramides are to be mimicked. In such experiments, the difference in physical properties pointed out in the present paper should not be overlooked.

Acknowledgments

This work was supported in part by the Spanish Ministerio de Ciencia y Tecnología (Grant No. BMC 2002-00784), and by the University of the Basque Country (Grant No. 9/UPV 00042.310-13552/2001). J.S. was a Predoctoral Fellow of the Basque Government.

References

[1] R.N. Kolesnick, A.E. Paley, 1,2-Diacylglycerols and phorbol esters stimulate phosphatidylcholine metabolism in GH3 pituitary cells. Evidence for separate mechanisms of action, J. Biol. Chem. 262 (1987) 9204–9210.

[2] T. Okazaki, R.M. Bell, Y.A. Hannun, Sphingomyelin turnover induced by vitamin D3 in HL-60 cells. Role in cell differentiation, J. Biol. Chem. 264 (1989) 19076–19080.
[3] R.N. Kolesnick, F.M. Goni, A. Alonso, Compartmentalization of ceramide signaling: physical foundations and biological effects, J. Cell. Physiol. 184 (2000) 285–300 (Review).
[4] A.E. Cremesti, F.M. Goni, R. Kolesnick, Role of sphingomyelinase and ceramide in modulating rafts: do biophysical properties determine biologic outcome? FEBS Lett. 531 (2002) 47–53.
[5] W.J. Van Blitterswijk, A. van der Luit, R.J. Veldman, M. Verheij, J. Borst, Ceramide: second messenger or modulator of membrane structure and dynamics? Biochem. J. 369 (2003) 199–211.
[6] C.G. Simon Jr, A.R. Gear, Membrane-destabilizing properties of C2-ceramide may be responsible for its ability to inhibit platelet aggregation, Biochemistry 37 (1998) 2059–2069.
[7] H.W. Huang, E.M. Goldberg, R. Zidovetzki, Ceramides perturb the structure of phosphatidylcholine bilayers and modulate the activity of phospholipase A2, Eur. Biophys. J. 27 (1998) 361–366.
[8] H.W. Huang, E.M. Goldberg, R. Zidovetzki, Ceramide induces structural defects into phosphatidylcholine bilayers and activates phospholipase A2, Biochem. Biophys. Res. Commun. 220 (1996) 834–838.
[9] H.W. Huang, E.M. Goldberg, R. Zidovetzki, Ceramides modulate protein kinase C activity and perturb the structure of phosphatidylcholine/phosphatidylserine bilayers, Biophys. J. 77 (1999) 1489–1497.
[10] J.M. Holopainen, J.Y. Lehtonen, P.K. Kinnunen, Lipid microdomains in dimyristoylphosphatidylcholine-ceramide liposomes, Chem. Phys. Lipids 88 (1997) 1–13.
[11] J.M. Holopainen, M. Subramanian, P.K. Kinnunen, Sphingomyelinase induces lipid microdomain formation in a fluid phosphatidylcholine/sphingomyelin membrane, Biochemistry 37 (1998) 17562–17570.
[12] M.P. Veiga, J.L. Arrondo, F.M. Goni, A. Alonso, Ceramides in phospholipid membranes: effects on bilayer stability and transition to nonlamellar phases, Biophys. J. 76 (1999) 342–350.
[13] D.C. Carrer, B. Maggio, Phase behavior and molecular interactions in mixtures of ceramide with dipalmitoylphosphatidylcholine, J. Lipid Res. 40 (1999) 1978–1989.
[14] D.C. Carrer, S. Hartel, H.L. Monaco, B. Maggio, Ceramide modulates the lipid membrane organization at molecular and supramolecular levels, Chem. Phys. Lipids 122 (2003) 147–152.
[15] E. Gulbins, S. Dreschers, B. Wilker, H. Grassme, Ceramide, membrane rafts and infections, J. Mol. Med. 82 (2004) 357–363.
[16] M. London, E. London, Ceramide selectively displaces cholesterol from ordered lipid domains (rafts): implications for lipid raft structure and function, J. Biol. Chem. 279 (2004) 9997–10004.
[17] D.M. Small, Surface and bulk interactions of lipids and water with a classification of biologically active lipids based on these interactions, Fed. Proc. 29 (1970) 1320–1326.
[18] A. Helenius, K. Simons, Solubilization of membranes by detergents, Biochim. Biophys. Acta 415 (1975) 29–79.
[19] J. Slavik, Anilinonaphthalene sulphonate as a probe of membrane composition and function, Biochim. Biophys. Acta 694 (1982) 1–25.
[20] J.A. Killian, B. de Kruijff, Thermodynamic, motional and structural aspects of gramicidin-induced hexagonal H_{II} phase formation in phosphatidylethanolamine, Biochemistry 24 (1985) 7881–7890.
[21] P. Sanchez-Pinera, F.J. Aranda, V. Micol, A. de Godos, J.C. Gomez-Fernandez, Modulation and polymorphic properties of dielaidoyl-phosphatidylethanolemine by the antineoplastic ether lipid 1-0-octadecyl-2-0-methyl-glycero-3-phosphocholine, Biochim. Biophys. Acta 1417 (1999) 202–210.
[22] D. Marsh, Lateral pressure in membranes, Biochim. Biophys. Acta 1286 (1996) 183–223 (Review).
[23] J.B. Massey, Interaction of ceramides with phosphatidylcholine, sphingomyelin and sphingomyelin/cholesterol bilayers, Biochim. Biophys. Acta 1510 (2001) 167–184.
[24] T.C. Lee, M.C. Ou, K. Shinozaki, B. Malone, F. Snyder, Biosynthesis of *N*-acetylsphingosine by platelet-activating factor: sphingosine CoA-independent transacetylase in HL-60 cells, J. Biol. Chem. 271 (1996) 209–217.
[25] J.A. Hamilton, D.M. Small, Solubilization and localization of triolein in phosphatidylcholine bilayers: a ^{13}C NMR study, Proc. Natl. Acad. Sci. U. S. A. 78 (1981) 6878–6882.
[26] J.M. Smaby, H.L. Brockman, Regulation of cholesteryl oleate and triolein miscibility in monolayers and bilayers, J. Biol. Chem. 262 (1987) 8206–8212.
[27] C.G. Simon Jr, P.W. Holloway, A.R. Gear, Exchange of C(16)-ceramide between phospholipid vesicles, Biochemistry 38 (1999) 14676–14682.
[28] S. Mathias, L.A. Pena, RN. Kolesnick, Signal transduction of stress via ceramide, Biochem. J. 335 (1998) 465–480.
[29] R. Guidoni, G. Sala, A. Giuliani, Use of sphingolipid analogs: benefits and risks, Biochim. Biophys. Acta 1439 (1999) 17–39.
[30] A.W. Adamson, Physical Chemistry of Surfaces, 3rd edition, Wiley, New York, 1976.
[31] H. Brockman, Lipid monolayers: why use half a membrane to characterize protein–membrane interactions? Curr. Opin. Struck. Biol. 9 (1999) 438–443.
[32] M. Di Paola, T. Cocco, M. Lorusso, Ceramide interaction with the respiratory chain of heart mitochondria, Biochemistry 39 (2000) 6660–6668.
[33] F.M. Goni, M.A. Requero, A. Alonso, Palmitoylcarnitine, a surface-active metabolite, FEBS Lett. 390 (1996) 1–5 (Review).
[34] J. Sot, M.I. Collado, J.L.R. Arrondo, A. Alonso, F.M. Goñi, Triton X-100-resistant bilayers: effect of lipid composition and relevance to the raft phenomenon, Langmuir 18 (2002) 2828–2835.
[35] M.A. Urbaneja, A. Alonso, J.M. Gonzalez-Mañas, F.M. Goni, M.A. Partearroyo, M. Tribout, S. Paredes, Detergent solubilization of phospholipid vesicle. Effect of electric charge, Biochem. J. 270 (1990) 305–308.